



Article

Anti-Windup Pitch Angle Control for Wind Turbines Based on Bounded Uncertainty and Disturbance Estimator

Xuguo Jiao ^{1,2} , Guozhong Wang ¹ , Xin Wang ^{3,4}, Zhenyong Zhang ^{5,*}, Yanbing Tian ¹ and Xiwen Fan ¹

¹ School of Information and Control Engineering, Qingdao University of Technology, Qingdao 266520, China; jiaoxuguo@qut.edu.cn (X.J.); guobiao8883@126.com (G.W.); tianyanbing@qut.edu.cn (Y.T.); evinzakeluc@outlook.com (X.F.)

² State Key Laboratory of Industrial Control Technology, College of Control Science and Engineering, Zhejiang University, Hangzhou 310027, China

³ Key Laboratory of Computing Power Network and Information Security, Ministry of Education, Shandong Computer Science Center, Qilu University of Technology, Shandong Academy of Sciences, Jinan 250014, China; xinwang@qlu.edu.cn

⁴ Shandong Provincial Key Laboratory of Computer Networks, Shandong Fundamental Research Center for Computer Science, Jinan 250014, China

⁵ State Key Laboratory of Public Big Data, College of Computer Science and Technology, Guizhou University, Guiyang 550025, China

* Correspondence: zyzhangnew@gmail.com

Abstract: Due to physical limitations and safety requirements, the rate and amplitude of change in wind turbines' pitch angle are limited, which will bring integral saturation problems to the control system. This leads to the deterioration of the pitch control system's performance or even an instability problem. This paper designs an anti-windup robust pitch angle control strategy to deal with pitch rate constraint issue to enhance the safety of the control system. First, to facilitate controller design, a filtered tracking-error technique is employed to transform the nonaffine form into an affine one. Subsequently, a feedback robust controller based on an uncertainty and disturbance estimator (UDE) is developed to handle the model's uncertainty and external disturbances. To address the issue of integral saturation in the pitch system and guarantee its safety, an elliptical bounded constraint is integrated into the designed UDE strategy. This bounded UDE controller can improve the stability of power generation quality, reducing the mechanical loads on components. Finally, the effectiveness of the proposed scheme is verified on the Wind Turbine Blockset platform in Matlab/Simulink. It can achieve better performance than traditional methods.

Keywords: variable speed wind turbine (VSWT); pitch angle control; integral saturation; bounded uncertainty and disturbance estimator (UDE)



Citation: Jiao, X.; Wang, G.; Wang, X.; Zhang, Z.; Tian, Y.; Fan, X.

Anti-Windup Pitch Angle Control for Wind Turbines Based on Bounded Uncertainty and Disturbance Estimator. *J. Mar. Sci. Eng.* **2024**, *12*, 473. <https://doi.org/10.3390/jmse12030473>

Academic Editors: Dong-Sheng Jeng, Rafael Morales and Eva Segura

Received: 6 February 2024

Revised: 2 March 2024

Accepted: 8 March 2024

Published: 10 March 2024



Copyright: © 2024 by the authors. Licensee MDPI, Basel, Switzerland. This article is an open access article distributed under the terms and conditions of the Creative Commons Attribution (CC BY) license (<https://creativecommons.org/licenses/by/4.0/>).

1. Introduction

In recent years, environmental pollution has garnered widespread attention from an increasing number of countries worldwide [1]. As using the traditional fossil energy seriously pollutes the environment, the global power grid is transforming from traditional fossil energy to clean energy. Since wind energy is one of the clean energies with huge reserves, wind power is developing rapidly around the world [2]. According to the forecast report published by the International Renewable Energy Agency (IRENA), wind power will play a main role in power generation by 2050 [3].

Variable-speed wind turbines (VSWTs) are widely used in modern wind farms, thanks to their ability to capture more wind energy and the mechanical load being at a lower level compared with fixed-speed turbines [1]. To maximize wind power capture as much as possible, the height and size of VSWTs are becoming larger and larger, which will increase structural loads, bring safety issues and make the system be more fragile in extreme uncertain wind conditions [4]. Therefore, how to develop intelligent control technologies

to achieve safe operation and loads optimization in wind turbines remains a challenging yet promising issue within the field of wind power.

Uneven turbulent winds easily generate fluctuations in power generation, increasing the difficulty of grid integration [5], and VSWTs cannot withstand high rotor speeds and torques in extreme environments [6]. When the rotor speed is bigger than its rated value, the pitch angle is adjusted to maintain constant power output. The aerodynamic torque can fluctuate a lot when a minor angle variation occurs, and thus, the pitch angle is closely related to the power output. Due to the high sensitivity with aerodynamic torque, the randomness and uncertainty of wind speed bring great challenges for advanced pitch angle control design.

Many control strategies for pitch angle have been proposed by scholars in order to achieve a good control performance. Proportional–integral–derivative (PID) controllers play an important role in VSWT pitch angle control [7]. However, due to the great sensitivity of nonlinear aerodynamics to the pitch angle, a constant PI gain cannot achieve an effective control effect [8]. Jason et al. [9] propose a gain-scheduled PI blade-pitch controller which measures the sensitive degree between aerodynamic power and different pitch angles and performs linear regression processing on it. In this way, the gain coefficient is adjusted according to the real-time pitch angle to achieve a better control effect. Atif et al. [10] use a particle swarm optimization (PSO) algorithm based on *fminsearch* to obtain the optimal parameters for PID and have demonstrated in experiments that this method can achieve more stable speed performance than traditional PID methods. However, the aging of components and the accumulation of waste on the blades can lead to changes in the aerodynamic power–pitch angle relationship, and thus, it will reduce the control effectiveness in practice. To deal with this, Billel et al. [11] proposed a direct power control based on PI control using space vector modulation technology, and optimizes the gain of PI control using a root optimization algorithm, improving the stability of wind turbine power generation. Furthermore, Ibrahim et al. [12] have developed a fractional order PID (FOPID) variable pitch controller based on oppositional brain storm optimization (OBSTO). The parameters of the FOPID controller are effectively selected by the OBSTO algorithm, improving control performance in various aspects.

The above methods do not consider the problem of integral saturation of PI-based pitch controllers, which can lead to system instability and increase mechanical loads while wind turbines are operational, especially in extreme uncertain wind conditions [13,14]. In wind turbines, the pitch angle actuator has physical limitations and safety requirements, which restricts the extent and the pitch angle variable rate. When the controller output exceeds the actuator's limit, there is a discrepancy between the actuator input and the controller output. This discrepancy causes the integral effect in the controller to continually accumulate, leading to integral saturation [15]. This saturation results in a decline in control function and it may even cause the system to lose the original control [16,17].

In order to address integral saturation, an integral saturation judgment module is typically added. When integral saturation occurs, applying a reverse gain can obviate the cumulative values of the corresponding parameters [18]. Nevertheless, the robustness of the system cannot be ensured by this method. Another approach is to use a more complex anti-integration and saturation design [19], but this requires additional calculations of system architecture. Sachin et al. [20] propose a neural fuzzy PID (NF-PID) control strategy, which can react quickly to change in wind speed and mitigate the negative impact of integral saturation on performance. Comparative experiments prove the superiority of NF-PID in pitch adjustment. Leith and Leithead [21] highlight the problem of blade-pitch integral saturation during turbines' operation, and several anti-integral saturation designs are compared. Garelli et al. [22] address the issue of pitch-rate integral saturation by adding a module to counteract saturation and adjusting the reference signal. Validation of this approach is conducted on a small-scale wind turbine. Kanev and van Engelen [23] propose a solution to integral saturation in controllers by introducing an auxiliary loop to adjust the

input signal. However, these methods involve additional auxiliary anti-integral saturation components, and their effectiveness in ensuring overall system stability remains uncertain.

Recently, the UDE-based control theory has achieved great development in control communities [24]. It shows good performance in dealing with robust control for nonlinear uncertain systems [25]. Therefore, under the excitation of the UDE control strategy, this paper develops an anti-windup pitch control scheme for VSWT based on the bounded UDE. This article makes the following specific contributions:

- By modeling the wind turbine and using filtered regulation error technique, the control signal is converted into an affine form that is suitable for controller design. A pitch angle controller based on the UDE is utilized to handle uncertainties and disturbances in the system, enhancing the overall system’s robustness and feasibility of the proposed controller for different types of turbines.
- A constraint coefficient is designed to solve the integration saturation problem that occurs in the traditional UDE. Integrating the elliptical bounded constraint with the UDE control framework, a bounded UDE approach is developed. This strategy enhances power generation stability, declines the corresponding mechanical load to a certain extent, and improves overall system safety. Moreover, this controller maintains the traditional UDE method’s robustness and clear system structure without requiring additional calculations.
- Simulation analyses are carried out by using a professional wind turbine platform to demonstrate the effectiveness of the proposed control strategy, and it can achieve better control performance compared with traditional methods.

The arrangement of this paper is as follows. Section 2 establishes the model of VSWT. Section 3 determines the control objectives and uses the filtered regulation error technique to convert a non-affine system into an affine one. Section 4 provides a detailed analysis of the design of the control controller and demonstrates its stability. Simulation result analyses are carried out in Section 5. Finally, Section 6 offers the conclusion of this study.

2. VSWT Modeling

Figure 1 displays the physical model of the VSWT under consideration. According to Betz Law [26], the aerodynamic power P_a captured by a wind turbine from flowing air can be expressed as

$$P_a = \frac{1}{2} \rho_1 \pi R^2 C_p(\lambda, \beta) v^3, \tag{1}$$

where ρ_1 represents the air density, R is the radius of the swept area of the wind turbine rotor, v represents the effective wind speed, λ represents tip speed ratio, and β is the pitch angle. The power coefficient C_p describes the wind power capture efficiency of wind turbines. It is a non-linear function determined by λ and β . λ can be described as

$$\lambda = \frac{R\omega_r}{v}, \tag{2}$$

with ω_r being the rotor speed. In general, the value of $C_p(\lambda, \beta)$ can be determined through a large number of experiments implemented by manufacturers [27]. Moreover, the aerodynamic torque can be represented as

$$T_a = \frac{1}{2} \rho \pi R^3 C_q(\lambda, \beta) v^2, \tag{3}$$

with $C_q(\lambda, \beta)$ being the torque coefficient, whose expression is

$$C_q(\lambda, \beta) = \frac{C_p(\lambda, \beta)}{\lambda}. \tag{4}$$

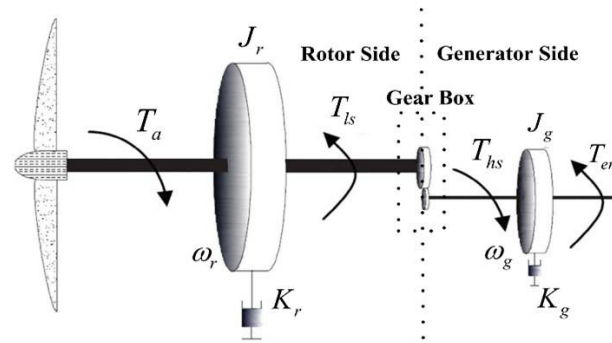


Figure 1. Physical model of VSWT.

In this research, the dual-mass structure of the VSWT is considered, assuming that the rotor-side and the generator-side drive shafts are rigid [28]. Furthermore, based on the fundamental laws of physics, the dynamic characteristics of the system can be represented as

$$\begin{cases} J_r \dot{\omega}_r = T_a - K_r \omega_r - T_{ls} \\ J_g \dot{\omega}_g = T_{hs} - K_g \omega_g - T_{em} \\ n_g = \frac{\omega_g}{\omega_r} = \frac{T_{ls}}{T_{hs}} \end{cases}, \tag{5}$$

where J_r and J_g are, respectively, the inertial constants of rotor and generator, ω_g denotes the generator speed, T_{ls} and T_{hs} are torques of high-speed and low-speed shafts, respectively, K_r and K_g are, respectively, external damping coefficients of wind rotor and generator, and n_g is the ratio of gearbox.

Further, considering that the nonlinear turbine system always operates in an uncertain operating environment [29], $d(t)$ is introduced to represent the unmodeled dynamics and unknown disturbance [30]. Therefore, the mathematical expression of the wind turbine model can be simplified as [9,31]

$$\dot{\omega}_r = \frac{1}{J_t} T_a - \frac{1}{J_t} K_t \omega_r - \frac{1}{J_t} T_g + d(t), \tag{6}$$

where J_t , K_t and T_g are the lumped terms whose specific expressions are

$$\begin{cases} J_t = n_g^2 J_g + J_r \\ K_t = n_g^2 K_g + K_r \\ T_g = n_g T_{em} \end{cases} \tag{7}$$

Finally, the output power of the generator in a VSWT can be represented as

$$P_g = T_g \omega_r. \tag{8}$$

3. Control Objectives

It can be observed from Figure 2 that three regions can be segmented for the operating stage of VSWT based on different wind speed values (Regions 1–3) [32]. In Region 2, the main control goal is to capture more energy from the flowing air. The rotor speed is adjusted by controlling the generator torque to achieve this control goal [33]. In Region 3, there are two main control objectives. Firstly, in this stage, when wind energy is relatively large, the windup issue with the pitch controller may destabilize the system’s operation, posing a significant risk of safety incidents involving the wind turbine generator. To guarantee the turbines’ safe operation, rotor speed and power generation must remain stable close to their rated values. Secondly, to minimize the wind turbine system’s failure rates, the mechanical loads of its key components should be minimized as much as possible to extend turbines’ service life.

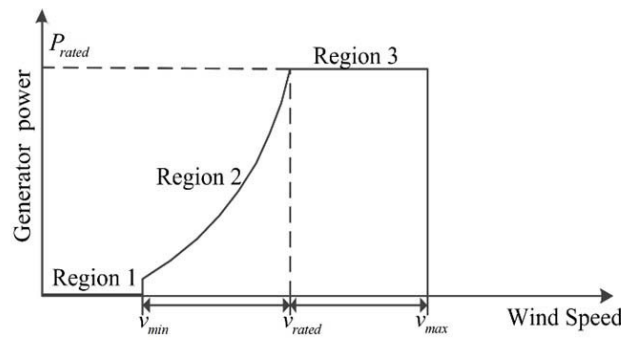


Figure 2. Operating regions of VSWT.

Under high wind speeds, the usual practice is to set the approach generator torque T_g to a fixed value. By controlling the change in the pitch angle β , the rotor speed ω_r is stable near the rated speed ω_d to realize the constant power output. The rotor speed regulation error can be described as

$$e = \omega_r - \omega_d. \tag{9}$$

Conclusions from (3) and (6) indicate that the system dynamics are influenced by the signal β in a non-affine manner, posing significant challenges in designing the appropriate controller [34]. To circumvent this issue, the filtered regulation error technology is employed to convert the control signal into an affine form. As a result, the regulation error r is defined as

$$r = c\dot{e} + e, \tag{10}$$

where $c > 0$. It can be seen that when $r \rightarrow 0$, e will also approach 0. The purpose of the controller designed for this study is to eliminate the adjustment error r and reduce the mechanical impacts of important parts.

4. Controller Design

4.1. The UDE-Based Controller

According to Equations (4) and (7), the derivative of the adjustment error is derived as follows

$$\begin{aligned} \dot{r} &= \frac{c}{J_t} (\dot{T}_a - \dot{T}_g - K_t \dot{\omega}_r + \dot{d}(t)) + \left(\frac{1}{J_t} T_a - \frac{K_t}{J_t} \omega_r - \frac{1}{J_t} T_g + d(t) \right) \\ &= f(\omega_r, v, \beta) + g(\omega_r, v, \beta) \dot{\beta} + \varphi(t), \end{aligned} \tag{11}$$

where

$$f(\omega_r, v, \beta) = \frac{c}{J_t} \left[\frac{\partial T_a}{\partial \omega_r} \left(\frac{T_a}{J_t} - \frac{K_t}{J_t} \omega_r - \frac{T_g}{J_t} \right) - \frac{K_t}{J_t} (T_a - K_t \omega_r - T_g) \right] + \left(\frac{1}{J_t} T_a - \frac{K_t}{J_t} \omega_r - \frac{1}{J_t} T_g \right), \tag{12}$$

$$g(\omega_r, v, \beta) = \frac{c}{J_t} \frac{\partial T_a}{\partial \beta} < 0, \tag{13}$$

$$\varphi(t) = \left(\frac{c}{J_t^2} \frac{\partial T_a}{\partial \omega_r} - \frac{c K_t}{J_t^2} + \frac{1}{J_t} \right) d(t) + \frac{c}{J_t} \dot{d}(t) + \frac{c}{J_t} \frac{\partial T_a}{\partial v} \dot{v}. \tag{14}$$

To compensate for system uncertainties and disturbances, Equation (11) can be rewritten as

$$\dot{r} = f_d(\omega_r, v_d, \beta) + g_d(\omega_r, v_d, \beta) \dot{\beta} + D(t), \tag{15}$$

where $D(t) = (f - f_d) + (g - g_d) + \varphi(t)$, and since the wind speed is known, f_d and g_d can be calculated by the wind turbine dynamic model as

$$f_d = \frac{c}{J_{td}} \left[\frac{\partial T_{ad}}{\partial \omega_r} \left(\frac{T_{ad}}{J_{td}} - \frac{K_{td}}{J_{td}} \omega_r - \frac{T_g}{J_{td}} \right) - \frac{K_{td}}{J_{td}} (T_{ad} - K_{td} \omega_r - T_g) \right] + \frac{1}{J_{td}} (T_{ad} - K_{td} - T_g), \tag{16}$$

$$g_d = \frac{c}{J_{td}} \frac{1}{2\lambda_d} \rho \pi R^3 v_d^2 c_{1d} \left(\left(-\frac{1}{\lambda_{id}^2} \frac{\partial \lambda_{id}}{\partial \beta} - c_{3d} \right) e^{-\frac{c_{5d}}{\lambda_{id}}} + \left(\frac{c_{2d}}{\lambda_{id}} - c_{3d}\beta - c_{4d} \right) e^{-\frac{c_{5d}}{\lambda_{id}}} \frac{c_{5d}}{\lambda_{id}^2} \frac{\partial \lambda_{id}}{\partial \beta} \right), \quad (17)$$

where $c_{1d} - c_{6d}$ is the coefficient provided by the manufacturer related to capture efficiency and

$$\frac{\partial T_{ad}}{\partial \omega_r} = \frac{1}{2} \rho \pi R^3 v_d^2 \left[\left(c_{1d} \left(-\frac{1}{\lambda_{id}^2} \right) \left(\frac{\partial \lambda_{id}}{\partial \omega_r} \right) e^{-\frac{c_{5d}}{\lambda_{id}}} \left(c_{2d} - c_{5d} \left(\frac{c_{2d}}{\lambda_{id}} - c_{3d}\beta - c_{4d} \right) \right) + c_{6d} \frac{R}{v_d} \right) \lambda_d - C_{pd}(\lambda_d, \beta) \frac{R}{v_d} \right] / \lambda_d^2. \quad (18)$$

In order for r to approach 0, the filtering error should satisfy the following relationship:

$$\dot{r}(t) = -kr(t), \quad (19)$$

where $k > 0$, and the control rate of the control signal is designed as

$$\dot{\beta} = -\frac{1}{g_d} (f_d + kr + D(t)). \quad (20)$$

When the system uncertainty and disturbance $D(t)$ are unknown, based on the UDE theoretical analysis, they are approximated as

$$\begin{aligned} \hat{D}(t) &= D(t) * g_f(t) \\ &= (\dot{r} - f_0 - g_0 \hat{\beta}) * g_f(t). \end{aligned} \quad (21)$$

In this formula, $g_f(t)$ is a filter with appropriate bandwidth, and “*” is the symbol for convolution. Combined with Equation (20), it can be obtained that

$$\dot{\beta} = -\frac{1}{g_d} \left(f_d + (\dot{r} - f_d - g_d \dot{\beta}) * g_f(t) + kr \right), \quad (22)$$

and arranging Equation (22) gives

$$-g_d \dot{\beta} = f_d + \dot{r} * g_f(t) - f_d * g_f(t) - g_d \dot{\beta} * g_f(t) + kr. \quad (23)$$

A Laplace transform is performed on both sides of the equation in Equation (23), simplified and an inverse Laplace transform is performed. The pitch angle control rate based on UDE is represented as

$$\dot{\beta} = -\frac{1}{g_d} \left(f_d + L^{-1} \left(\frac{1}{1 - G_f(s)} \right) * kr + L^{-1} \left(\frac{sG_f(s)}{1 - G_f(s)} \right) * r \right), \quad (24)$$

where L^{-1} is the operator for Laplace inverse transformation, and $G_f(s)$ usually uses a first-order low-pass filter, which can be expressed as

$$G_f(s) = \frac{1}{\tau s + 1}. \quad (25)$$

According to Equation (25), Equation (24) can be further deduced as

$$\dot{\beta} = -\frac{1}{g_d} \left(f_d + \frac{k}{\tau} \int_0^t r(\zeta) d\zeta + \left(\frac{1}{\tau} + k \right) r(t) \right). \quad (26)$$

4.2. Design with Bounded Constraints

In the UDE control signal (26), the integral term generated by the characteristics of the filter exists in the $\left(\frac{1}{1 - G_f(s)} \right)$ term. The integral term continuously corrects the tracking error

to achieve good steady-state tracking performance. In fact, due to the non-ideal physical structure of VSWTs, the rate of change in the pitch is bounded. When the input of the actuator exceeds the limit, the traditional UDE controller would erroneously update the state, causing the accumulation of the integral term during the error-adjustment process. It will then lead to integral saturation. This phenomenon will result in a deterioration in control performance. To alleviate the continuous impact of the integral action, a time-varying variable is designed for Equation (19) as

$$\dot{r}(t) = -k_0kr(t), \tag{27}$$

with $0 < k_0 < 1$. If the controller output is close to the boundary of the pitch angle change rate, k_0 should be close to 0 to avoid integral saturation. The pitch angle change rate range can be expressed as

$$\dot{\beta} \in (\dot{\beta}_{\min}, \dot{\beta}_{\max}). \tag{28}$$

The boundary values of the pitch angle change rates, $\dot{\beta}_{\min}$ and $\dot{\beta}_{\max}$, are both constants, and the values are determined by the physical limitations and safety requirements of the actuator. In order to constrain the process, an elliptic relationship shown in Figure 3 can be established between the pitch angle change rate $\dot{\beta}$ and the constraint coefficient k_0 as

$$\frac{4(\dot{\beta} - \frac{\dot{\beta}_{\max} + \dot{\beta}_{\min}}{2})^2}{(\dot{\beta}_{\max} - \dot{\beta}_{\min})^2} + k_0^2 = 1 \tag{29}$$

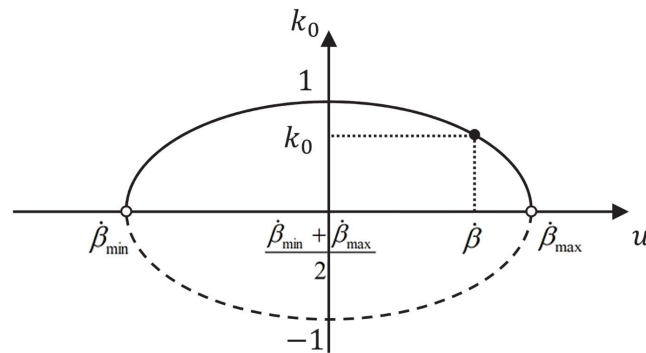


Figure 3. The elliptical relationship between the rate of the pitch angle and the constraint coefficients.

According to the new filter error dynamics, the pitch angle control rate is modified as

$$\dot{\beta}_n = -\frac{1}{g_0}(f_0 + (\frac{1}{\tau} + k)r(t) + \frac{k_0k}{\tau} \int_0^t r(\zeta)d\zeta). \tag{30}$$

Further, to realize the required constraint model, a pitch controller with bounded constraints is invented for the time-varying constraint coefficients and final controller output as

$$\dot{k}_0 = -k_1k_0(\frac{4(\dot{\beta} - \frac{\dot{\beta}_{\max} + \dot{\beta}_{\min}}{2})^2}{(\dot{\beta}_{\max} - \dot{\beta}_{\min})^2} + k_0^2 - 1) + \frac{4k_2(\dot{\beta} - \frac{\dot{\beta}_{\max} + \dot{\beta}_{\min}}{2})}{(\dot{\beta}_{\max} - \dot{\beta}_{\min})^2}k_0(\dot{\beta} - \dot{\beta}_n), \tag{31}$$

$$\ddot{\beta} = -k_1(\dot{\beta} - \frac{\dot{\beta}_{\max} + \dot{\beta}_{\min}}{2}) \cdot (\frac{4(\dot{\beta} - \frac{\dot{\beta}_{\max} + \dot{\beta}_{\min}}{2})^2}{(\dot{\beta}_{\max} - \dot{\beta}_{\min})^2} + k_0^2 - 1) - k_2k_0^2(\dot{\beta} - \dot{\beta}_n), \tag{32}$$

where $\dot{\beta}$ is the input of the pitch actuator, k_0 is the constraint coefficient of the introduction of the integral term, and k_1 and k_2 are positive constants. It should be noted that the bounded controller design only needs to occupy very little computing resources in the

achievement of the bounded constraints. The control diagram of the proposed bounded UDE is shown in Figure 4.

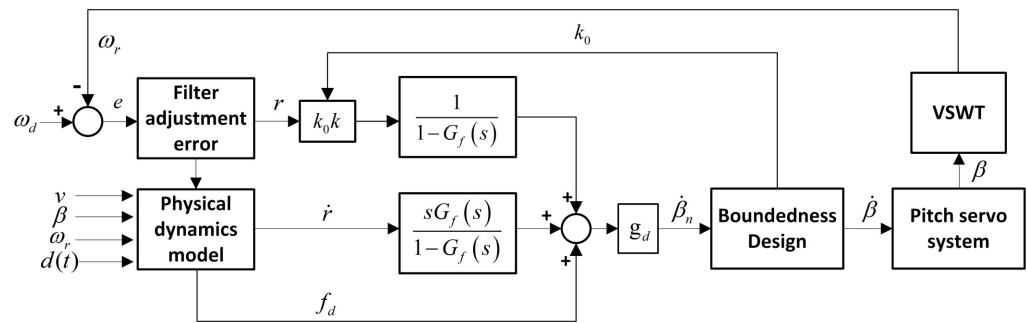


Figure 4. The framework of the bounded UDE pitch angle control method.

4.3. Proof of Stability

The proof of stability considers the following Lyapunov function candidates:

$$V(t) = \frac{4(\dot{\beta} - \frac{\dot{\beta}_{\max} + \dot{\beta}_{\min}}{2})^2}{(\dot{\beta}_{\max} - \dot{\beta}_{\min})^2} + k_0^2. \tag{33}$$

According to Equations (31) and (32), the derivative of Equation (33) is taken as

$$\dot{V}(t) = -2k_1 V^2(t) + 2k_1 V(t). \tag{34}$$

Further solving Equation (34) gives

$$V(t) = \frac{1}{1 - \left(1 - \frac{1}{V(0)}\right) e^{-2k_1 t}}, \tag{35}$$

where $V(0)$ is the initial state of $V(t)$, through the initial design of $V(0) = 1$, $k_0(0) = 1$ and $\dot{\beta}(0) = \frac{\dot{\beta}_{\max} + \dot{\beta}_{\min}}{2}$ can be obtained, and then,

$$V(t) = 1 \quad \forall t \geq 0. \tag{36}$$

In Equation (33), as long as $\forall t \geq 0$, the controller output and constraint coefficients will always remain within the ellipse defined by Equation (29), ensuring system stability. With the proposed bounded design, both $\dot{\beta}$ and k_0 will always remain on the ellipse set, regardless of their changes in Equation (30). In the steady state, the derivatives of the control signal change rate and the constraint coefficient will be adjusted to 0, and the tracking error e is zero. At this point, both the pitch angle and the constraint coefficient will approach a stable point (β_e, k_{0e}) . The bounded design scheme of the controller based on UDE is illustrated in Figure 4.

5. Simulation Verification

The designed pitch controller’s regulation function is proven on the Matlab/Simulink Wind Turbine Blockset platform [35]. The platform focuses on wind power study and provides very good help for related technology research. It receives funding from the Danish Energy Agency in the study program “A Simulation Platform to Model, Optimize and Design Wind Turbines” and has been extensively utilized in the related literature [31,36,37]. The model used on this platform is 1.5 MW VSWT. Table 1 introduces the primary data used in the study [38]. When the pitch acceleration is too high, the contact stress of the bearings will increase, resulting in increased friction, wear and fatigue [39]. When the run time is long, this may lead to damage and failure of the bearing, which will affect the normal and safe operation of the entire VSWT and seriously affect the economic benefits of the wind

farm. In an effort to make a reasonable analysis of the influence extent of the controller on the pitch mechanical shock (PMS), the average pitch angle absolute acceleration of the entire running time of the fan can be measured. The smaller it is, the smaller the mechanical shock of the pitch control system. Furthermore, to evaluate blade pitch fatigue (PF) during operation, the following indicators need to be considered [40].

$$PF = \frac{\sum_{k=1}^{T_{et}} |\beta(k+1) - \beta(k)|}{T_{et}} \tag{37}$$

PF measures the average blade pitch variation rate during operation. Clearly, a smaller PF value indicates less fatigue in the pitch control system [41]. In order to analyze integral saturation states more intuitively, scheduling parameters are introduced in this study as [42]

$$r = \frac{\text{sat}_r(u)}{u}, \quad r = 1 \text{ if } u = 0, \tag{38}$$

where the numerator is the implemented pitch rate by the actuator, and the denominator is the pitch rate signal output by the controller. When integral saturation is not present, the value of r is equal to 1. The parameters for the designed controller are chose as $k = 3$, $c_{1d} = 0.5176$, $c_{2d} = 116$, $c_{3d} = 0.4$, $c_{4d} = 5$, $c_{5d} = 21$, $c_{6d} = 0.0068$, $\tau = 2.5$, $c = 4.5$, $k_1 = 18.6$ and $k_2 = 15.5$. In an effort to simulate extreme conditions, the pitch rate suffers from a limitation, and the limited range is set as ± 3 deg/s in simulations.

In addition, classic gain anti-windup methods are introduced in traditional UDE [18,43]. This method feedbacks the difference between the input and output of the actuator to the integrator, and the gain coefficient selected in this comparative experiment is 0.55. The control strategy for gain anti-saturation UDE is shown in Figure 5. Furthermore, under different wind conditions, simulation analysis is conducted on bounded UDE, traditional UDE and gain anti-windup UDE.

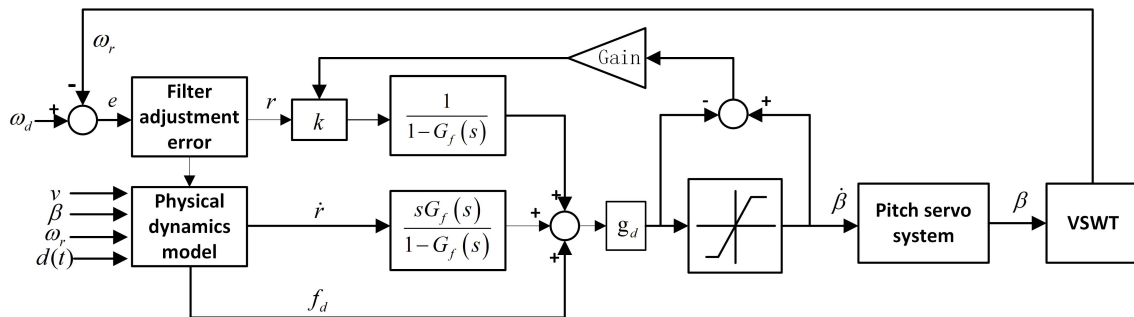


Figure 5. The framework of the gain anti-windup pitch angle control method.

Table 1. Main parameters of the simulation model.

Parameters	Value	Parameters	Value
Air density	1.25 kg/m ³	Rated power	1.5 MW
Gearbox ratio	83.531	Generator rated torque	8376 N · m
Wind rotor's external damping coefficient	45.52 N·m/(rad·s)	Generator's external damping coefficient	0.4 N·m/(rad·s)
Cut-out wind speed	25 m/s	Cut-in wind speed	3 m/s
Inertial constant of generator	90 kg·m ²	Rotor radius	40 m
Inertial constant of rotor	4,950,000 kg·m ²	Rated speed	2.1423 rad/s

5.1. Wind Gust

In an effort to prove the validity of the bounded UDE method under extreme wind scenarios, the gust model is built as follows [18,44]:

$$v = \begin{cases} 16, t < T_{in} \\ 16 + A_g[1 - \cos(\frac{2\pi(t-T_{in})}{D_g})], T_{in} \leq t \leq T_{out} \\ 16, T_{out} < t \end{cases} , \quad (39)$$

where $T_{in} = 10$ s, $T_{out} = 17.5$ s, $A_g = 4.5$ m/s and $D_g = 7.5$ s are the entry time, exit time, amplitude value and duration of the gust. Figure 6a shows the generated gust wind speed. The comparison of the experimental conclusions of the three controllers when gust is shown in Figure 6b–f. To contrast the speed regulation performance and the pitch loads, refer to the performance index shown in Table 2. These include the mean absolute error (MAE), standard deviation (ST), mean absolute percentage error (MAPE), pitch mechanical shock (PMS) and pitch fatigue (PF) from the rated value. The speed regulation performance of the bounded UDE is superior to the conventional UDE and gain anti-windup UDE in terms of MAE, with a reduction of 41.59% and 6.16%, respectively. Figure 6e,f depict the actuator saturation states and the accumulation of integrators under three control strategies. Evidently, the bounded UDE eliminates the infinite accumulation of integral terms caused by integral saturation, and no integral saturation phenomenon occurs. The integrator in traditional UDE methods experiences significant accumulation, leading the system into an uncontrollable state during this period. The system remains in this state until the integral term is eliminated. The gain anti-windup UDE method can eliminate partial saturation, but the introduction of negative gain reduces control performance. The significant impact of bounded constraints can be observed in Figure 6d, where better control performance is achieved with fewer blade pitch adjustments. PMS and PF are indicators directly affecting the turbine’s lifespan, and the bounded UDE reduces them by 40.29% and 36.15%, respectively, compared with the traditional UDE method. Compared with the gain anti-windup UDE method, the bounded UDE is reduced by 17.34% and 7.50%, respectively. This improvement enhances the safety and extends the service life of turbines, which is very beneficial for wind farm’s economic benefits.

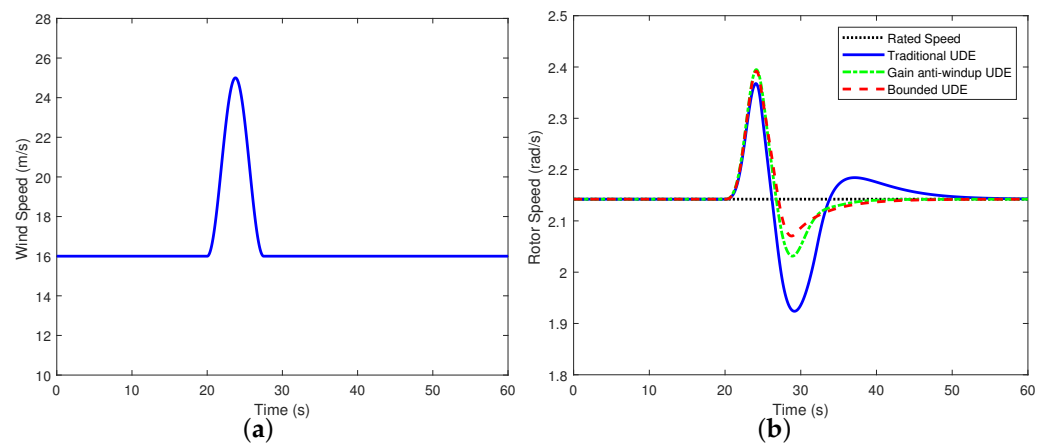


Figure 6. Cont.

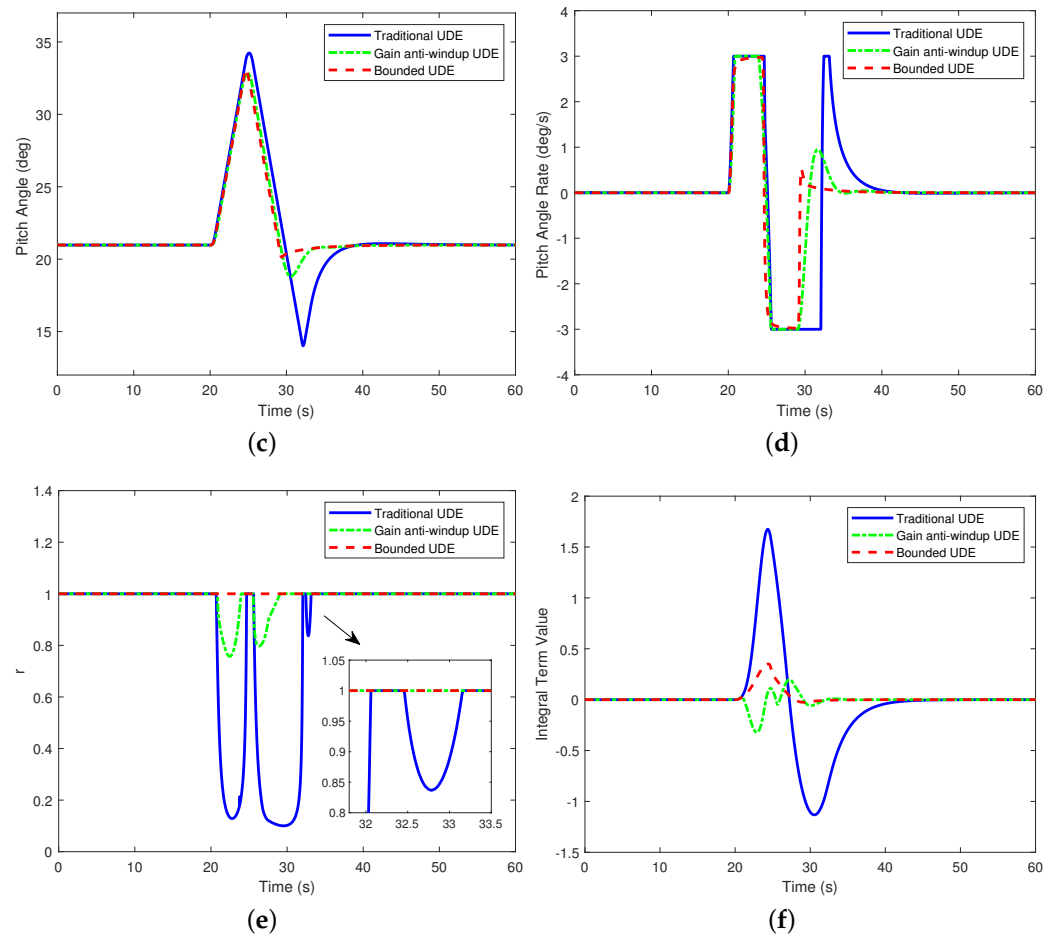


Figure 6. Simulation results of VSWT under gust conditions. (a) Wind speed–time relationship. (b) Rotor speed. (c) Pitch angles. (d) Pitch angle rate. (e) The saturation states of the actuators. (f) The integral terms.

Table 2. Performance metrics of three controllers under gust conditions.

	MAE (rad/s)	ST (rad/s)	MAPE (%)	PMS (rad/s ²)	PF (rad/s)
Traditional UDE	0.0339	0.0693	1.6133	1.0000	1.0000
Gain anti-windup UDE	0.0211	0.0546	0.9528	0.7224	0.6903
Bounded UDE	0.0198	0.0512	0.8842	0.5971	0.6385

5.2. Step Wind

The designed method’s effectiveness can be testified by the step wind scene [45]. Under the airflow velocity shown in Figure 7a, the simulation results of important parameters of the controller are shown in Figure 7b–f. By analyzing the obtained experiment results, the control performance indicators are shown in Table 3. It is known that the pitch rate adjustment of the traditional UDE is rapid. Between 20 s and 35 s, the pitch rate surpasses the boundary value of the actuator, leading to integral saturation and consequently causing an increase in the time to reach steady state. The bounded UDE eliminates integral saturation, and the signals of the controller and the actuator remain synchronized throughout the operation. During a stable wind speed, the pitch angle under the bounded UDE control strategy approaches the stable value in a shorter time. Based on the experimental results, the bounded UDE method, compared to the traditional and the gain anti-windup approach, exhibits a reduction of 6.74% and 11.7% in MAE, respectively. This suggests that the bounded UDE method provides more stable speed control performance. Similarly,

the bounded design demonstrates excellent performance in integral saturation. In Figure 7c, the blades of the bounded UDE exhibit no unnecessary pitch adjustments. Through the calculation of pitch fatigue, the bounded UDE has similar effects to the gain-anti-saturation UDE, with a reduction of 8.68% compared to the traditional UDE.

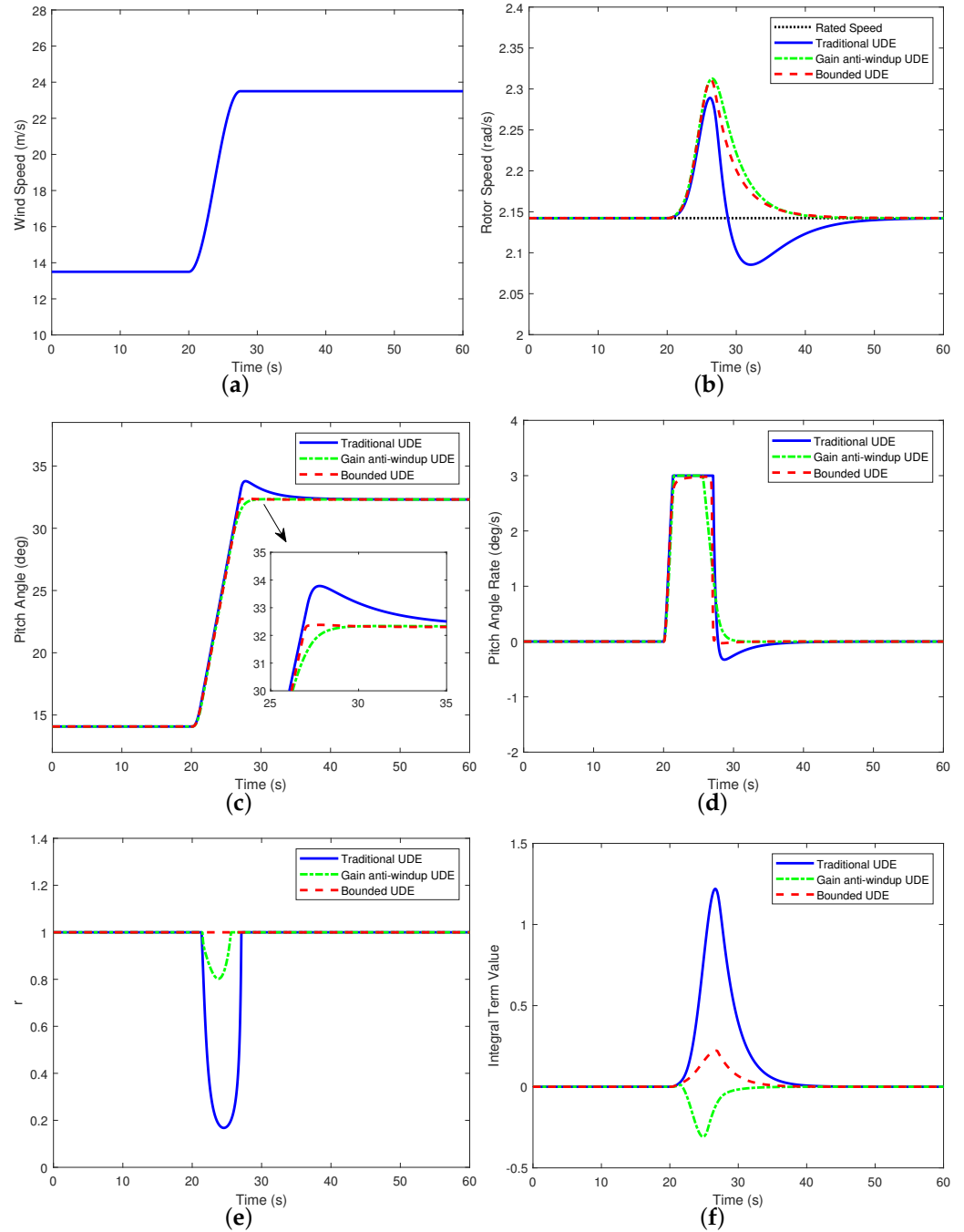


Figure 7. Simulation results of VSWT under step conditions. (a) Wind speed–time relationship. (b) Rotor speed. (c) Pitch angles. (d) Pitch angle rate. (e) The saturation states of the actuators. (f) The integral terms.

Table 3. Performance metrics of three controllers under step conditions.

	MAE (rad/s)	ST (rad/s)	MAPE (%)	PMS (rad/s ²)	PF (rad/s)
Traditional UDE	0.0178	0.0359	0.8195	1.0000	1.0000
Gain anti-windup UDE	0.0188	0.0454	0.8345	0.8676	0.9101
Bounded UDE	0.0166	0.0408	0.7415	0.7026	0.9132

5.3. Turbulent Wind

The functionality of the controller designed in this paper is greatly proved using long-term turbulent winds in this part [18,45]. The wind speed information shown in Figure 8a is generated by TurbSim (Version 1.06.00) software [46,47]. In the turbulent wind scenario, Figure 8b–Figure 8d, respectively, display the performance of speed regulation and pitch adjustment under different controllers. It can be observed that the speed of bounded UDE and traditional UDE quickly stabilizes near the rated value, and the gain anti-windup method increases the oscillation of the control signal, resulting in significant speed overshoot. The actual wind conditions in the environment exhibit randomness and intermittency, as shown between 120 s and 140 s in Figure 8a. In Figure 8e,f, the saturation state indicator r of the conventional UDE proves that the controller’s output signal has exceeded the actuator’s boundaries. The controller’s state is continuously updated erroneously, and the integral term keeps accumulating. When the wind speed undergoes a significant abrupt change, the larger integral term hinders the correct adjustment of the controller’s output signal. As seen in Figure 8c,d, the conventional UDE regains the controller’s tracking capability after the elimination of the integral term. During the operation of the wind turbine, controller instability can subject the system to substantial shocks, potentially leading to wind turbine safety accidents. The bounded UDE constrains the unlimited accumulation of the integral term, ensuring that the actuator saturation state remains within normal bounds. This approach achieves superior speed tracking with fewer pitch actions. To evaluate the controller’s performance more clearly, Table 4 provides a detailed analysis of the experiment results. Compared with the traditional UDE and gain reverse saturation UDE, the bounded UDE reduces MAE by 1.37% and 27.06%, while PF decreases by 3.83% and 2.13%, respectively. The simulation results clearly indicate that the bounded UDE not only ensures enhanced tracking performance but also reduces the loads on pitch systems.

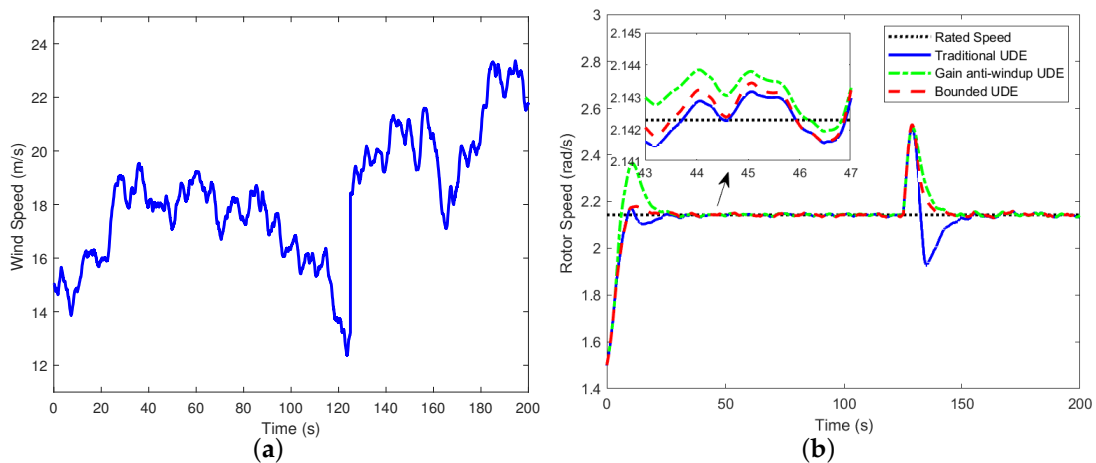


Figure 8. Cont.

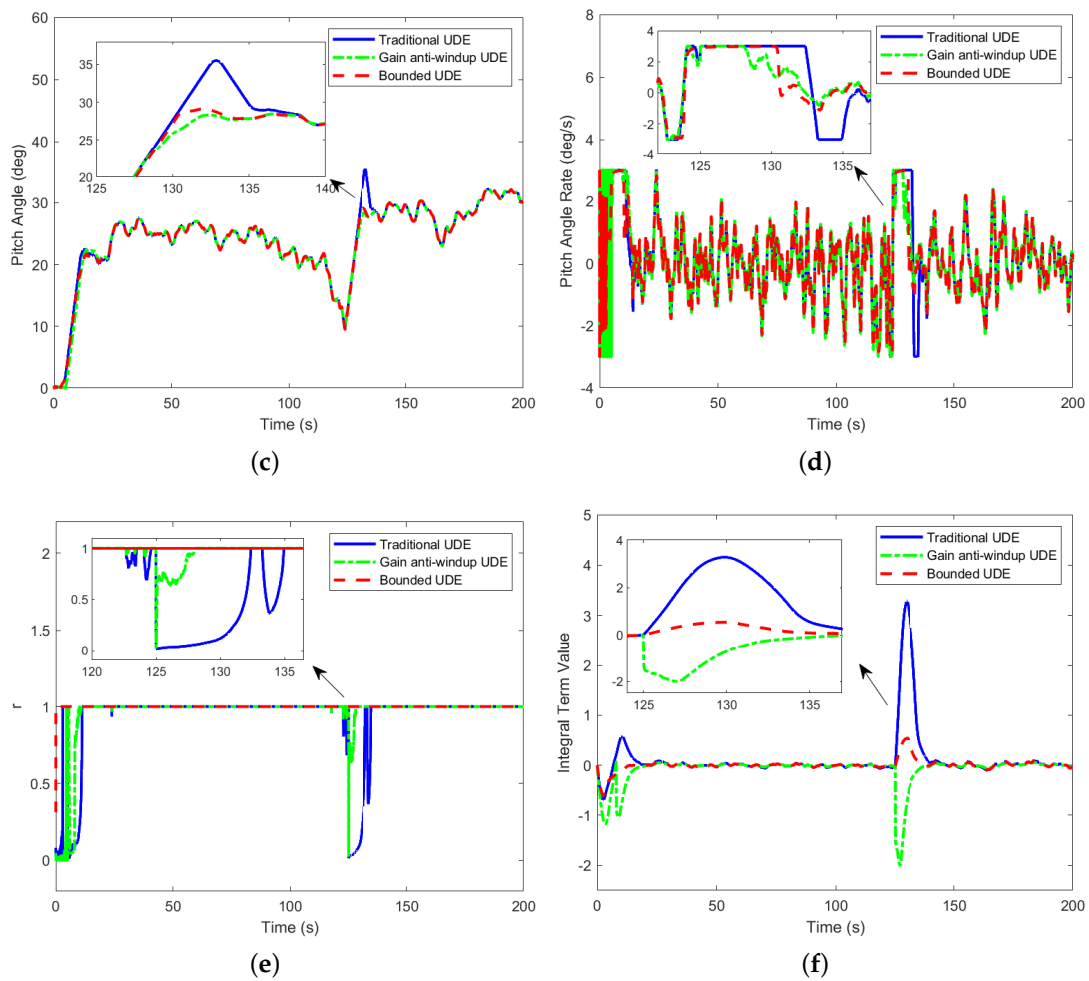


Figure 8. Simulation results of VSWT under under turbulent wind conditions. (a) Wind speed–time relationship. (b) Rotor speed. (c) Pitch angles. (d) Pitch angle rate. (e) The saturation states of the actuators. (f) The integral terms.

Table 4. Performance metrics of three controllers under turbulent conditions.

	MAE (rad/s)	ST (rad/s)	MAPE (%)	PMS (rad/s ²)	PF (rad/s)
Traditional UDE	0.0511	0.1372	2.9191	1.0000	1.0000
Gain anti-windup UDE	0.0691	0.1021	3.6397	1.4325	0.9617
Bounded UDE	0.0504	0.1376	2.8890	0.8858	0.9412

6. Conclusions

This paper proposes a robust bounded UDE pitch control strategy, which is intended to optimize the power generation quality of wind turbines at high wind speeds, reduce mechanical fatigues and enhance the turbine’s safety. First, a UDE-based pitch control is introduced to address the system’s uncertainties. In order to eliminate the integral saturation that occurs in the designed UDE control, an elliptic bounded constraint coefficient is investigated. As a result, when integral saturation occurs, the integral action is weakened, and the integral saturation is eliminated. Based on the bounded constrained design, a bounded UDE pitch angle controller is developed. It is worth noting that the design with bounded constraints will not increase the computational complexity of the system. Simulation results can prove that the bounded UDE control method has better performance in reducing the mechanical fatigue of pitch systems with good rotor speed

regulation results than conventional UDE. It will reduce maintenance costs, extend the life of the turbines and enhance the overall system's safety.

Author Contributions: Methodology, X.J., Z.Z. and X.W.; Software, G.W.; Validation, X.J. and X.W.; Investigation, X.J. and X.W.; Resources, Z.Z., Y.T. and X.F.; Data curation, G.W.; Writing—review and editing, X.J. and G.W.; Project administration, Z.Z., Y.T. and X.F. All authors have read and agreed to the published version of the manuscript.

Funding: This work was supported in part by the National Natural Science Foundation of China under Grant 62203249, Grant 62303126 and Grant 62362008, in part by the Shandong Provincial Nature Science Foundation of China under Grant ZR2021QF115, in part by the Lixian Scholar Project of Qingdao University of Technology, in part by the Open Research Project of the State Key Laboratory of Industrial Control Technology, Zhejiang University, China, under Grant ICT2023B08, in part by the Taishan Scholars Program under Grant tsqn202211203, and in part by the “20 New Universities” Project of Jinan City under Grant 202228077.

Data Availability Statement: The data are unavailable due to privacy security.

Conflicts of Interest: The authors declare that they have no conflicts of interest to report regarding the present study.

References

- Jiao, X.; Yang, Q.; Xu, B. Hybrid intelligent feedforward-feedback pitch control for VSWT with predicted wind speed. *IEEE Trans. Energy Convers.* **2021**, *36*, 2770–2781. [\[CrossRef\]](#)
- Ismaeel, A.; Houssein, E.H.; Hassan, A.Y.; Said, M. Performance of gradient-based optimizer for optimum wind cube design. *Comput. Mater. Contin.* **2022**, *71*, 339–353.
- IRENA. *Renewable Capacity Statistics*; International Renewable Energy Agency (IRENA): Abu Dhabi, United Arab Emirates, 2020.
- Liu, W.; Su, X.; An, Y.; Huang, K. Local buckling prediction for large wind turbine blades. *Comput. Mater. Contin.* **2011**, *25*, 177.
- Shirkhani, M.; Tavoosi, J.; Danyali, S.; Sarvenoe, A.K.; Abdali, A.; Mohammadzadeh, A.; Zhang, C. A review on microgrid decentralized energy/voltage control structures and methods. *Energy Rep.* **2023**, *10*, 368–380. [\[CrossRef\]](#)
- Marouani, H.; Almealmadi, F.A.; Farkh, R.; Dhahri, H. Wind Turbine Efficiency Under Altitude Consideration Using an Improved Particle Swarm Framework. *Comput. Mater. Contin.* **2022**, *73*, 4981–4994. [\[CrossRef\]](#)
- Shah, K.A.; Meng, F.; Li, Y.; Nagamune, R.; Zhou, Y.; Ren, Z.; Jiang, Z. A synthesis of feasible control methods for floating offshore wind turbine system dynamics. *Renew. Sustain. Energy Rev.* **2021**, *151*, 111525. [\[CrossRef\]](#)
- Elkodama, A.; Ismaiel, A.; Abdellatif, A.; Shaaban, S.; Yoshida, S.; Rushdi, M.A. Control methods for horizontal axis wind turbines (HAWT): State-of-the-art review. *Energies* **2023**, *16*, 6394. [\[CrossRef\]](#)
- Jonkman, J.; Butterfield, S.; Musial, W.; Scott, G. *Definition of a 5-MW Reference Wind Turbine for Offshore System Development*; Technical report; National Renewable Energy Lab. (NREL): Golden, CO, USA, 2009.
- Iqbal, A.; Ying, D.; Saleem, A.; Hayat, M.A.; Mateen, M. Proposed particle swarm optimization technique for the wind turbine control system. *Meas. Control.* **2020**, *53*, 1022–1030. [\[CrossRef\]](#)
- Meghni, B.; Benamor, A.; Hachana, O.; Azar, A.T.; Boulmaiz, A.; Saad, S.; El-kenawy, E.S.M.; Kamal, N.A.; Fati, S.M.; Bahgaat, N.K. Rooted Tree Optimization for Wind Turbine Optimum Control Based on Energy Storage System. *Comput. Mater. Contin.* **2023**, *74*, 3977. [\[CrossRef\]](#)
- Mehedi, I.M.; Al-Saggaf, U.M.; Vellingiri, M.T.; Milyani, A.H.; Bin Saad, N.; Bin Yahaya, N.Z. OBSO Based Fractional PID for MPPT-Pitch Control of Wind Turbine Systems. *Comput. Mater. Contin.* **2022**, *71*, 4001–4017. [\[CrossRef\]](#)
- Zhao, S.; Yang, Q.; Cheng, P.; Deng, R.; Xia, J. Adaptive resilient control for variable-speed wind turbines against false data injection attacks. *IEEE Trans. Sustain. Energy* **2022**, *13*, 971–985. [\[CrossRef\]](#)
- Wang, Z.; Zhang, H.; Cao, X.; Liu, E.; Li, H.; Zhang, J. Modeling and Detection Scheme for Zero-Dynamics Attack on Wind Power System. *IEEE Trans. Smart Grid* **2023**, *15*, 934–943. [\[CrossRef\]](#)
- Bohn, C.; Atherton, D. An analysis package comparing PID anti-windup strategies. *IEEE Control Syst. Mag.* **1995**, *15*, 34–40.
- Konstantopoulos, G.C.; Zhong, Q.C.; Ren, B.; Krstic, M. Bounded integral control of input-to-state practically stable nonlinear systems to guarantee closed-loop stability. *IEEE Trans. Autom. Control* **2016**, *61*, 4196–4202. [\[CrossRef\]](#)
- Tarbouriech, S.; Turner, M. Anti-windup design: An overview of some recent advances and open problems. *IET Control Theory Appl.* **2009**, *3*, 1–19. [\[CrossRef\]](#)
- Inthamoussou, F.A.; Bianchi, F.D.; De Battista, H.; Mantz, R.J. LPV wind turbine control with anti-windup features covering the complete wind speed range. *IEEE Trans. Energy Convers.* **2014**, *29*, 259–266. [\[CrossRef\]](#)
- Beltran, B.; Ahmed-Ali, T.; Benbouzid, M.E.H. Sliding mode power control of variable-speed wind energy conversion systems. *IEEE Trans. Energy Convers.* **2008**, *23*, 551–558. [\[CrossRef\]](#)
- Goyal, S.; Deolia, V.K.; Agrawal, S. An Advanced Neuro-Fuzzy Tuned PID Controller for Pitch Control of Horizontal Axis Wind Turbines. *ECTI Trans. Electr. Eng. Electron. Commun.* **2022**, *20*, 296–305. [\[CrossRef\]](#)

21. Leith, D.J.; Leithead, W. Implementation of wind turbine controllers. *Int. J. Control* **1997**, *66*, 349–380. [[CrossRef](#)]
22. Garelli, F.; Camocardi, P.; Mantz, R.J. Variable structure strategy to avoid amplitude and rate saturation in pitch control of a wind turbine. *Int. J. Hydrog. Energy* **2010**, *35*, 5869–5875. [[CrossRef](#)]
23. Kanev, S.; van Engelen, T. Exploring the limits in individual pitch control. In Proceedings of the European Wind Energy Conference, Marseille, France, 16–19 March 2009; pp. 16–19.
24. Ren, B.; Zhong, Q.C. UDE-based robust control of variable-speed wind turbines. In Proceedings of the 39th Annual Conference of the IEEE Industrial Electronics Society (IECON 2013), Vienna, Austria, 10–13 November 2013; pp. 3818–3823.
25. Wang, Y.; Ren, B.; Zhong, Q.C. Bounded UDE-based controller for input constrained systems with uncertainties and disturbances. *IEEE Trans. Ind. Electron.* **2020**, *68*, 1560–1570. [[CrossRef](#)]
26. Rauh, A.; Seelert, W. The Betz optimum efficiency for windmills. *Appl. Energy* **1984**, *17*, 15–23. [[CrossRef](#)]
27. Yang, Q.; Jiao, X.; Luo, Q.; Chen, Q.; Sun, Y. L1 adaptive pitch angle controller of wind energy conversion systems. *ISA Trans.* **2020**, *103*, 28–36. [[CrossRef](#)] [[PubMed](#)]
28. Bianchi, F.D.; De Battista, H.; Mantz, R.J. *Wind Turbine Control Systems: Principles, Modelling and Gain Scheduling Design*; Springer: London, UK, 2007; Volume 19.
29. Jiao, X.; Sun, Y.; Ying, Y.; Yang, Q. Effective wind speed estimation based maximum power point tracking control for variable-speed wind turbine. In Proceedings of the 2017 Chinese Automation Congress (CAC), Jinan, China, 20–22 October 2017; pp. 6685–6690.
30. Luo, R.; Peng, Z.; Hu, J.; Ghosh, B.K. Adaptive optimal control of affine nonlinear systems via identifier-critic neural network approximation with relaxed PE conditions. *Neural Netw.* **2023**, *167*, 588–600. [[CrossRef](#)]
31. Zaragoza, J.; Pou, J.; Arias, A.; Spiteri, C.; Robles, E.; Ceballos, S. Study and experimental verification of control tuning strategies in a variable speed wind energy conversion system. *Renew. Energy* **2011**, *36*, 1421–1430. [[CrossRef](#)]
32. Shaltout, M.L.; Ma, Z.; Chen, D. An adaptive economic model predictive control approach for wind turbines. *J. Dyn. Syst. Meas. Control* **2018**, *140*, 051007. [[CrossRef](#)]
33. Zhao, L.; Chen, B.; Lu, J. Minimum Variance Control of Constant Power Output For Wind Energy Conversion System Above Rated Wind. In Proceedings of the 2010 Asia-Pacific Power and Energy Engineering Conference, Chengdu, China, 28–31 March 2010; pp. 1–4.
34. Guo, C.; Hu, J.; Hao, J.; Celikovskiy, S.; Hu, X. Fixed-time safe tracking control of uncertain high-order nonlinear pure-feedback systems via unified transformation functions. *arXiv* **2023**, arXiv:2305.00505.
35. Jiao, X.; Meng, W.; Yang, Q.; Fu, L.; Chen, Q. Adaptive continuous neural pitch angle control for variable-speed wind turbines. *Asian J. Control* **2019**, *21*, 1966–1979. [[CrossRef](#)]
36. Abbas, F.A.R.; Abdulsada, M.A. Simulation of wind-turbine speed control by MATLAB. *Int. J. Comput. Electr. Eng.* **2010**, *2*, 1793–8163. [[CrossRef](#)]
37. Hansen, M.H.; Zahle, F. *Aeroelastic Optimization of MW Wind Turbines*; Danmarks Tekniske Universitet, Risø Nationallaboratoriet for Bæredygtig Energi: Roskilde, Denmark, 2011.
38. Iov, F.; Hansen, A.D.; Sørensen, P.; Blaabjerg, F. *Wind Turbine Blockset in Matlab/Simulink-General Overview and Description of the Models*; Aalborg Universitet, Risø National Laboratory: Roskilde, Denmark, 2004.
39. Plumley, C.; Leithead, W.; Jamieson, P.; Bossanyi, E.; Graham, M. Comparison of individual pitch and smart rotor control strategies for load reduction. *J. Phys. Conf. Ser.* **2014**, *524*, 012054. [[CrossRef](#)]
40. Jain, A.; Schildbach, G.; Fagiano, L.; Morari, M. On the design and tuning of linear model predictive control for wind turbines. *Renew. Energy* **2015**, *80*, 664–673. [[CrossRef](#)]
41. Hatami, A.; Moetafegh-Imani, B. Innovative adaptive pitch control for small wind turbine fatigue load reduction. *Mechatronics* **2016**, *40*, 137–145. [[CrossRef](#)]
42. Meisami-Azad, M.; Grigoriadis, K.M. Anti-windup linear parameter-varying control of pitch actuators in wind turbines. *Wind Energy* **2015**, *18*, 187–200. [[CrossRef](#)]
43. Wright, A.D.; Fingersh, L. *Advanced Control Design for Wind Turbines; Part I: Control Design, Implementation, and Initial Tests*; Technical report; National Renewable Energy Lab. (NREL): Golden, CO, USA, 2008.
44. Jiao, X.; Yang, Q.; Fan, B.; Chen, Q.; Sun, Y.; Wang, L. EWSE and uncertainty and disturbance estimator based pitch angle control for wind turbine systems operating in above-rated wind speed region. *J. Dyn. Syst. Meas. Control* **2020**, *142*, 031006. [[CrossRef](#)]
45. Song, D.; Yang, J.; Cai, Z.; Dong, M.; Su, M.; Wang, Y. Wind estimation with a non-standard extended Kalman filter and its application on maximum power extraction for variable speed wind turbines. *Appl. Energy* **2017**, *190*, 670–685. [[CrossRef](#)]
46. Jonkman, B.J. *TurbSim User's Guide*; Technical report; National Renewable Energy Lab. (NREL): Golden, CO, USA, 2006.
47. Xie, J.; Dong, H.; Zhao, X. Data-driven torque and pitch control of wind turbines via reinforcement learning. *Renew. Energy* **2023**, *215*, 118893. [[CrossRef](#)]

Disclaimer/Publisher's Note: The statements, opinions and data contained in all publications are solely those of the individual author(s) and contributor(s) and not of MDPI and/or the editor(s). MDPI and/or the editor(s) disclaim responsibility for any injury to people or property resulting from any ideas, methods, instructions or products referred to in the content.